JACS
JOURNAL OF THE AMERICAN CHEMICAL SOCIETY

Communication

pubs.acs.org/JACS

Nanoporous Poly(lactide) by Olefin Metathesis Degradation

Arthur Bertrand and Marc A. Hillmyer*

Department of Chemistry, University of Minnesota, 207 Pleasant Street SE, Minneapolis, Minnesota 55455-0431, United States

Supporting Information

ABSTRACT: We describe an approach to ordered nanoporous poly(lactide) that relies on self-assembly of poly(butadiene)−poly(lactide) (PB−PLA) diblock copolymers followed by selective degradation of PB using olefin metathesis. The block copolymers were obtained by a combination of anionic and ring-opening transesterification polymerizations. The molar mass of each block was tailored to target materials with either a lamellar or cylindrical microphase-separated morphology. Orientation of these nanoscale domains was induced in thin films and monolithic samples through solvent annealing and mechanical deformation, respectively. Selective degradation of PB was achieved by immersing the samples in a solution of Grubbs first-generation catalyst in cyclohexane, a nonsolvent for PLA. Successful elimination of PB was confirmed by size-exclusion chromatography and ^{1}H NMR spectroscopy. Direct imaging of the resulting nanoporous PLA was obtained by scanning electron microscopy.

Poly(lactide) (PLA) has been used in various technologies over the last several decades because of its renewable origins, degradability to nontoxic byproducts, and biocompatibility.[1,2] PLA's propensity to degrade under mild conditions also renders it an attractive polymer for the design of ordered nanoporous materials from block polymer precursors.[3] Self-assembly of PLA-containing block polymers leads to nanostructured morphologies dictated mainly by the block polymer composition. After selective etching of the PLA domains, nanoporous materials can be generated. The designer nature of nanoporous materials from block polymers has spurred much interest in the biomedical and separations fields.[3f,4] However, the typically hydrophobic and nondegradable nature of the matrix material can be limiting for ephemeral applications in aqueous environments. We envisioned that nanoporous PLA samples could be quite useful for applications that exploit PLA's established biocompatibility and biodegradation characteristics (e.g., drug delivery excipients, tissue scaffolding, implantable devices).

A diblock copolymer with PLA as the majority component and an etchable minority component would be a promising precursor for the generation of an ordered nanoporous and biodegradable material. Several groups have reported methods to degrade hydrophobic polymer blocks, but the treatments that are usually required (e.g., strongly acidic/basic media,[5] ozonolysis,[6] reactive ion etching,[7] or pyrolysis[8]) naturally limit their use to chemically resistant polymer matrices. In fact, we have shown that ozone can compromise the integrity of PLA in block polymer thin films.[6d] Here we report the design and preparation of ordered nanoporous samples of PLA by using olefin metathesis to selectively remove poly(butadiene) (PB) from a nanostructured PB−PLA block copolymer precursor (Figure 1).

Figure 1. Route to ordered nanoporous PLA by metathesis etching of a PB−PLA diblock copolymer.

PB−PLA diblock copolymers were obtained by a combination of anionic and ring-opening transesterification polymerizations [Figure S1 in the Supporting Information (SI)]. Two diblock copolymers were employed in this study: PB−PLA (17−40) and PB−PLA (14−53), where the numbers designate the molar masses (in kg mol^{-1}) of the constituent blocks (Table S1 in the SI). They were processed in a home-built channel die at 120 °C, a particularly efficient method for inducing microstructural orientation that is beneficial to both morphological determination and the generation of monolithic nanoporous materials (see the SI).[9] The resulting shear-oriented samples were obtained as small sticks with square cross sections (dimensions: 50 mm × 2 mm × 2 mm). This treatment facilitated morphological assignment by small-angle X-ray scattering (SAXS) and transmission electron microscopy (TEM) analysis.[3b]

Synchrotron SAXS analysis of oriented PB−PLA (17−40) at 25 °C revealed an intense principal reflection (q^* = 0.119 nm^{-1}) as well as multiple higher-order reflections positioned at $2q^*$, $3q^*$, and $4q^*$ characteristic of an ordered lamellar morphology (Figure 2a). For PB−PLA (14−53), the SAXS profile revealed a principal reflection (q^* = 0.111 nm^{-1}) with an additional broad peak centered around $q = \sqrt{7}q^*$ (Figure 2b). The presence of small peaks at $q = \sqrt{3}q^*$ and $q = \sqrt{4}q^*$ was consistent with a hexagonally packed cylindrical morphology. The low intensity of these peaks was likely due to form factor extinction (Figure S2).

Received: May 20, 2013
Published: July 19, 2013

   dx.doi.org/10.1021/ja4050532 | J. Am. Chem. Soc. 2013, 135, 10918−10921

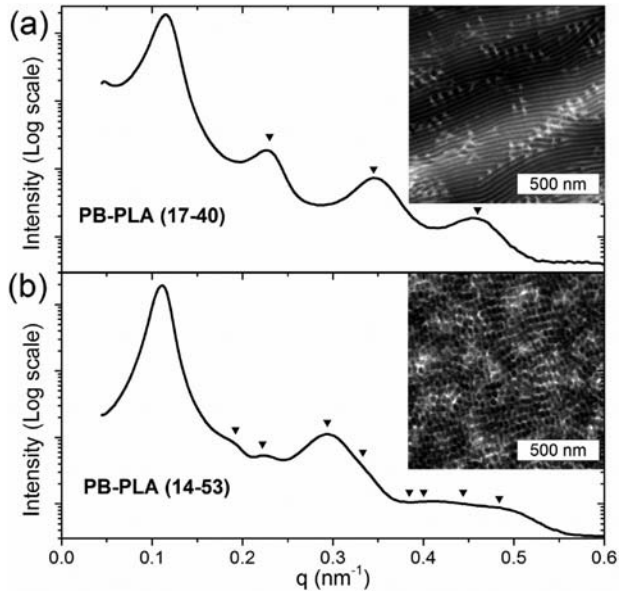

Figure 2. 1D SAXS profiles of shear-oriented PB−PLA samples at 25 °C. The triangle symbols indicate the expected reflections for (a) lamellar and (b) cylindrical morphologies. Insets: corresponding TEM images of the material, obtained perpendicular to the shear direction (PB domains were stained by OsO_4 vapors).

Further details concerning the SAXS results can be found in the SI (Figure S3).

TEM imaging of the aligned samples gave direct evidence of their ordered structures (Figures 2, S4, and S5). Although the morphology of PB−PLA (17−40) was lamellar, many defects were evident in the processed sample (Figure 2a inset). A discrepancy between the lamellar spacings estimated by TEM (42 nm) and SAXS (52.8 nm) was found, possibly arising from sample instability under the electron beam of the microscope. PB−PLA (14−53) was composed of cylinders oriented in the direction of the shear flow (Figure 2b inset). As in the case of the lamellar spacing of PB−PLA (17−40), the cylinder center-to-center distance measured for PB−PLA (14−53) by TEM (57 nm) was found to be somewhat smaller than the value obtained by SAXS (65 nm).

Russell and co-workers reported the formation of polyisoprene−PLA thin films containing perpendicular cylindrical PLA microdomains via solvent vapor annealing with chloroform.[10] Using a related procedure, thin films (∼65 nm) of cylinder-forming PB−PLA (14−53) on silicon wafers were prepared by spin-coating and exposed to a saturated chloroform atmosphere (see the SI). This process allowed the formation of well-defined PB cylinders oriented perpendicular and parallel to the surface, as evidenced by scanning electron microscopy (SEM) imaging (Figure S6). A well-organized hexagonally packed perpendicular cylindrical structure was achieved after 16 h of annealing, as evidenced by atomic force microscopy (AFM) imaging (Figure 3) and SEM imaging (Figure S7). Analysis of the AFM image in Figure 3a revealed an average cylinder diameter of 28 ± 6 nm (Figure S8). The cylinder center-to-center distance obtained by AFM (61 ± 7 nm) agreed well with the SAXS and TEM results (65 and 57 nm respectively). AFM images of a large area (16 μm^2) showed the long-range order that could be achieved (Figures S9 and S10).

Wagener and co-workers have demonstrated the degradation of 1,4-PB in the presence of a metathesis catalyst by

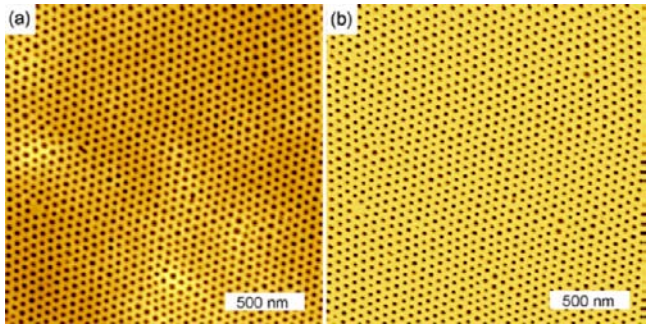

Figure 3. AFM images (2 μm × 2 μm, tapping mode) of a PB−PLA (14−53) thin film annealed for 16 h in a chloroform atmosphere: (a) height contrast; (b) phase contrast.

incorporation of the catalyst in the backbone, intramolecular cyclization, or cross-metathesis involving the 1,2 repeat units.[11] In particular, they showed that the degradation could be performed under solvent-free conditions: PB can dissolve solid catalyst placed on the polymer surface.[11c] The low-molar-mass species created by the metathesis then act as a solvent to facilitate further degradation.

In the present work, we aimed at selective degradation of nanoscale PB domains in a matrix of PLA that remains intact. Using a catalyst solution in a PB-selective solvent allows the catalyst to infiltrate into the PB domains while leaving the PLA matrix unaffected. Indeed, a nanoporous PLA thin film was prepared by immersing a piece (∼4 mm × 4 mm) of the well-aligned PB−PLA (14−53) thin film on a silicon wafer in a cyclohexane solution of Grubbs first-generation catalyst[12] for 15 h (see the SI).[13] The etched film was then uniformly coated with ∼1 nm Pt to allow SEM imaging with a pure topographic contrast. The micrograph of the etched film (Figure 4) revealed a nanoporous microstructure with dense hexagonal packing that spanned the entire surface of the sample, whereas a non-etched film exhibited an essentially flat surface (Figure S7b). Although some defects could be discerned, the fast Fourier transform of the SEM image was consistent with a well-organized hexagonal lattice. Image analysis revealed a narrow pore size distribution and after the Pt coating thickness was taken into account, an average pore diameter of 31 ± 4 nm and an average center-to-center distance of 59 ± 7 nm were determined; both values are in good accordance with those obtained from the AFM image before etching (see above). An SEM image representing a 50 μm^2 area demonstrated that the long-range order was preserved post etching (Figure S11). Cross-sectional SEM images of a cryofractured nanoporous thin film (Figures 4 and S12) showed that the cylindrical nanopores spanned the thin film. In addition, SEM images of Pt-coated nanoporous thin films that were subsequently scratched with a razor blade showed numerous hexagonally arranged bright spots on the surface of the exposed Si wafer (Figures S13 and S14). This clearly indicates deposition of Pt through the pores onto the substrate and confirms the fidelity of the pores from the top surface through to the substrate.

Preliminary attempts to degrade PB cylinders in shear-oriented PB−PLA (14−53) monoliths did not result in measurable PB loss, as determined by ^{1}H NMR spectroscopy and size-exclusion chromatography (SEC), presumably because of the lack of cylinder continuity throughout the sample (see Figure S4b). On the contrary, the degradation of PB lamellae in shear-oriented PB−PLA (17−40) was remarkably efficient. The etching of 180 mg of shear-oriented PB−PLA (17−40) resulted

dx.doi.org/10.1021/ja4050532 | J. Am. Chem. Soc. 2013, 135, 10918−10921

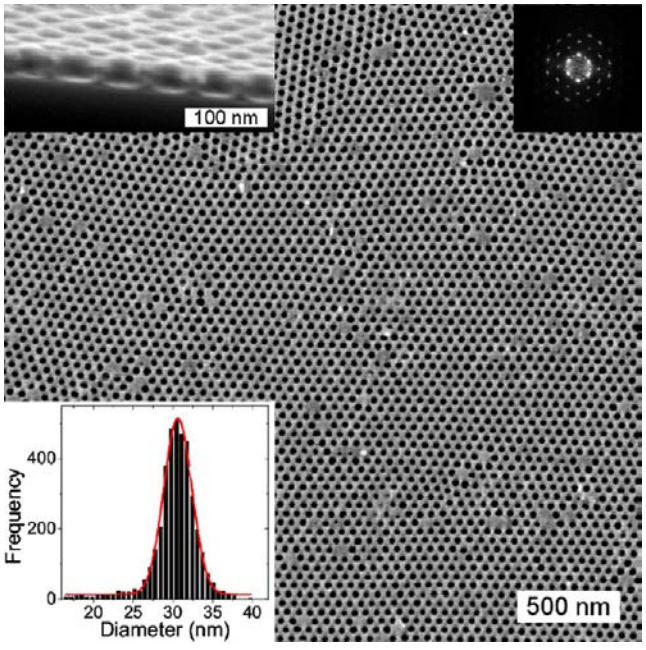

Figure 4. SEM image (10 μm^2) of a nanoporous PLA thin film obtained via selective etching of PB from PB−PLA (14−53) by metathesis. The sample was uniformly coated with ∼1 nm Pt. Insets: (top left) cross-sectional SEM image; (top right) Fourier transform; (bottom) pore size distribution after accounting for the ∼1 nm Pt coating. The solid line is a Gaussian fit yielding an average diameter of 31 ± 4 nm.

in a weight loss of 51 mg (−28 wt %), in good accordance with the calculated PB weight fraction in the PB−PLA precursor (30 wt %), and the PB resonances nearly completely (>95%) disappeared from the ^{1}H NMR spectrum after etching (Figure S15). SEC also showed a substantial decrease in molar mass after etching of the sample (Figure 5). However a small peak was

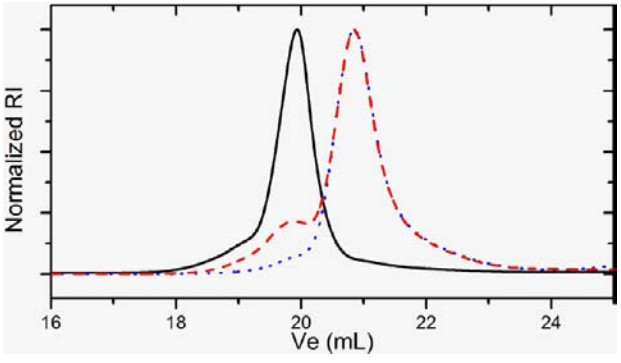

Figure 5. SEC traces of a shear-oriented PB−PLA (17−40) monolith in chloroform before metathesis (black solid line), after metathesis in cyclohexane (red dashed line), and after metathesis in chloroform (solution state) (blue dotted line).

visible at low elution volume (V_e), which we assigned to residual PB−PLA.[14] The refractive index increment (dn/dc) of PB in chloroform (0.083 mL g^{-1})[15] is 4 times higher than that of PLA (0.02 mL g^{-1}),[16] and by deconvolution of the SEC data the residual PB in the monolith was estimated to be ∼2 wt % (Figure S16). It is likely that some PB lamellae were fully surrounded by the PLA matrix and therefore were not accessible to the cyclohexane solution (see Figure 2a). This hypothesis was supported by the SEC analysis of a PB−PLA (17−40) sample that was fully dissolved in chloroform and metathetically degraded: no significant shoulder was observed at lower elution volume (Figure 5), and the remaining polymer was identified as pure PLA by ^{1}H NMR spectroscopy (Figure S15).[17]

Differential scanning calorimetry (DSC) thermograms of the etched monolithic sample revealed the absence of a PB glass transition (Figure S17). In addition, a small exothermic feature was observed near the PLA glass transition (∼55 °C) on the first heating cycle, whereas only the PLA glass transition was observed upon second heating. This feature was likely due to collapse of the microstructure, as reported previously.[3a,18] SAXS analysis showed a dramatic increase in the scattered intensity after etching due to the strong electron density contrast between the PLA and void domains (Figure S18). However, secondary peaks typical of a lamellar morphology were weaker in intensity. SEM imaging of the etched samples revealed the nanoporosity of the material (Figures 6 and S19). However, the lamellar micro-

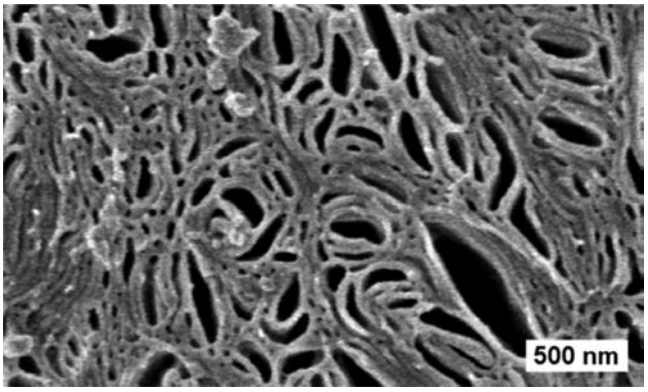

Figure 6. SEM image of a cryo-fractured PB−PLA (17−40) monolith after metathetic etching of the PB phase. The image was obtained perpendicular to the shear direction.

structure was clearly affected by the swelling/etching process; the pore-size distribution was particularly broad because of local pore collapse, as previously reported for porous lamellar structures.[8b,18] The total pore volume was estimated to be 0.41 mL g^{-1} on the basis of N_2 adsorption measurements at 77 K (Figure S20). This value is in good accordance with the theoretical pore volume calculated from the volume fractions of PB and PLA (0.425 mL g^{-1}), indicating a rather limited influence of the pore collapse. BET and BJH analysis gave a specific surface area of 34.4 m^2 g^{-1} and a mean "pore" diameter of 34 nm, respectively.

In summary, we have demonstrated the preparation of an ordered nanoporous and biodegradable material as both thin-film and monolithic samples. Clear evidence of selective PB degradation was provided by SEC and ^{1}H NMR analysis, while DSC, SAXS, N_2 adsorption, and SEM confirmed the resulting nanoporous structure of the material. Because of the biocompatibility and biosourced nature of PLA, such nanoporous PLA samples are promising materials for biomedical applications such as drug delivery, and strategies to prepare mechanically robust, free-standing membranes are amenable to our approach.[3f] In addition, the metathetic degradation of a polydiene constitutes a mild and straightforward method to prepare other synthetically challenging block-polymer-derived nanoporous materials.

dx.doi.org/10.1021/ja4050532 | J. Am. Chem. Soc. 2013, 135, 10918−10921

■ ASSOCIATED CONTENT

Supporting Information

Experimental procedures, PB−PLA copolymer properties (Table S1), and Figures S1−S20. This material is available free of charge via the Internet at http://pubs.acs.org.

■ AUTHOR INFORMATION

Corresponding Author

hillmyer@umn.edu

Notes

The authors declare no competing financial interest.

■ ACKNOWLEDGMENTS

This work was supported by the National Science Foundation (DMR-1006370). We thank Dr. Myungeun Seo for help with N_2 adsorption measurements and helpful input. We acknowledge Dr. Justin Kennemur, Dr. Justin Bolton, and Morgan Schulze for feedback on the manuscript. Parts of this work were carried out in the Characterization Facility, University of Minnesota, which receives partial support from NSF through the MRSEC and NNIN programs. Synchrotron SAXS data were obtained at the DuPont−Northwestern−Dow Collaborative Access Team (DND-CAT) located at Sector 5 of the Advanced Photon Source (APS). DND-CAT is supported by E.I. DuPont de Nemours & Co., The Dow Chemical Company, and Northwestern University. Use of the APS at Argonne national Laboratory was supported by the U. S. Department of Energy, Office of Science, Office of Basic Energy Sciences, under Contract No. DE-AC02-06CH11357.

■ REFERENCES

(1) (a) Okada, M. *Prog. Polym. Sci.* **2002**, *27*, 87. (b) Gupta, A. P.; Kumar, V. *Eur. Polym. J.* **2007**, *43*, 4053. (c) Gupta, A. P.; Kumar, V. *Eur. Polym. J.* **2007**, *43*, 4053. (d) Rasal, R. M.; Janorkar, A. V.; Hirt, D. E. *Prog. Polym. Sci.* **2010**, *35*, 338.

(2) (a) Ikada, Y.; Tsuji, H. *Macromol. Rapid Commun.* **2000**, *21*, 117. (b) Shum, H. C.; Kim, J.-W.; Weitz, D. A. *J. Am. Chem. Soc.* **2008**, *130*, 9543. (c) Kim, S.-H.; Shum, H. C.; Kim, J. W.; Cho, J.-C.; Weitz, D. A. *J. Am. Chem. Soc.* **2011**, *133*, 15165. (d) Oh, J. K. *Soft Matter* **2011**, *7*, 5096. (e) Samarajeewa, S.; Shrestha, R.; Li, Y.; Wooley, K. L. *J. Am. Chem. Soc.* **2011**, *134*, 1235. (f) Sinha Ray, S. *Acc. Chem. Res.* **2012**, *45*, 1710. (g) Ohya, Y.; Takahashi, A.; Nagahama, K. *Adv. Polym. Sci.* **2012**, *247*, 65.

(3) (a) Zalusky, A. S.; Olayo-Valles, R.; Wolf, J. H.; Hillmyer, M. A. *J. Am. Chem. Soc.* **2002**, *124*, 12761. (b) Rzayev, J.; Hillmyer, M. A. *J. Am. Chem. Soc.* **2005**, *127*, 13373. (c) Leiston-Belanger, J. M.; Russell, T. P.; Drockenmuller, E.; Hawker, C. J. *Macromolecules* **2005**, *38*, 7676. (d) Bolton, J.; Bailey, T. S.; Rzayev, J. *Nano Lett.* **2011**, *11*, 998. (e) Seo, M.; Hillmyer, M. A. *Science* **2012**, *336*, 1422. (f) Jackson, E. A.; Lee, Y.; Hillmyer, M. A. *Macromolecules* **2013**, *46*, 1484.

(4) (a) Querelle, S. E.; Chen, L.; Hillmyer, M. A.; Cussler, E. L.; Nijmeijer, K.; Wessling, M. *Ind. Eng. Chem. Res.* **2010**, *49*, 12051. (b) Ha, J.-M.; Wolf, J. H.; Hillmyer, M. A.; Ward, M. D. *J. Am. Chem. Soc.* **2004**, *126*, 3382. (c) Hamilton, B. D.; Weissbuch, I.; Lahav, M.; Hillmyer, M. A.; Ward, M. D. *J. Am. Chem. Soc.* **2009**, *131*, 2588.

(5) (a) Ndoni, S.; Vigild, M. E.; Berg, R. H. *J. Am. Chem. Soc.* **2003**, *125*, 13366. (b) Cavicchi, K. A.; Zalusky, A. S.; Hillmyer, M. A.; Lodge, T. P. *Macromol. Rapid Commun.* **2004**, *25*, 704. (c) Uehara, H.; Yoshida, T.; Kakiage, M.; Yamanobe, T.; Komoto, T.; Nomura, K.; Nakajima, K.; Matsuda, M. *Macromolecules* **2006**, *39*, 3971.

(6) (a) Lee, J. S.; Hirao, A.; Nakahama, S. *Macromolecules* **1988**, *21*, 274. (b) Hashimoto, T.; Tsutsumi, K.; Funaki, Y. *Langmuir* **1997**, *13*, 6869. (c) Okumura, A.; Nishikawa, Y.; Hashimoto, T. *Polymer* **2006**, *47*, 7805. (d) Guo, S.; Rzayev, J.; Bailey, T. S.; Zalusky, A. S.; Olayo-Valles, R.; Hillmyer, M. A. *Chem. Mater.* **2006**, *18*, 1719. (e) Smith, D. R.; Meier, D. J. *Polymer* **1992**, *33*, 3777.

(7) Chao, C.-C.; Wang, T.-C.; Ho, R.-M.; Georgopanos, P.; Avgeropoulos, A.; Thomas, E. L. *ACS Nano* **2010**, *4*, 2088.

(8) (a) Hedrick, J.; Labadie, J.; Russell, T.; Hofer, D.; Wakharker, V. *Polymer* **1993**, *34*, 4717. (b) Kosonen, H.; Valkama, S.; Nykänen, A.; Toivanen, M.; ten Brinke, G.; Ruokolainen, J.; Ikkala, O. *Adv. Mater.* **2006**, *18*, 201.

(9) Drzal, P. L.; Barnes, J. D.; Kofinas, P. *Polymer* **2001**, *42*, 5633.

(10) (a) Cavicchi, K. A.; Berthiaume, K. J.; Russell, T. P. *Polymer* **2005**, *46*, 11635. (b) Cavicchi, K. A.; Russell, T. P. *Macromolecules* **2007**, *40*, 1181.

(11) (a) Marmo, J. C.; Wagener, K. B. *Macromolecules* **1993**, *26*, 2137. (b) Marmo, J. C.; Wagener, K. B. *Macromolecules* **1995**, *28*, 2602. (c) Watson, M. D.; Wagener, K. B. *Macromolecules* **2000**, *33*, 1494.

(12) Trnka, T. M.; Grubbs, R. H. *Acc. Chem. Res.* **2000**, *34*, 18.

(13) We were also able to achieve PB etching in 1 h at room temperature, as evidenced by SEM (Figure S14).

(14) Performing the metathesis reaction for a longer time with a new catalyst solution did not improve the metathetic etching of PB. Trial use of *cis*-3-hexene as chain-transfer agent (CTA) turned out to be counterproductive, leaving a nearly unaffected polymer sample. We believe that competitive metathesis occurs between CTA molecules in the solution, decreasing the degradation rate of the material and leading to early decomposition of the catalyst, as suggested elsewhere: Thanki, P. N.; Reyx, D.; Campistron, I.; Laguerre, A.; Singh, R. P. *Eur. Polym. J.* **2004**, *40*, 2611.

(15) Tsoukatos, T.; Avgeropoulos, A.; Hadjichristidis, N.; Hong, K.; Mays, J. W. *Macromolecules* **2002**, *35*, 7928.

(16) Wang, L.; Jing, X.; Cheng, H.; Hu, X.; Yang, L.; Huang, Y. *Ind. Eng. Chem. Res.* **2012**, *51*, 10731.

(17) Mahanthappa, M. K.; Bates, F. S.; Hillmyer, M. A. *Macromolecules* **2005**, *38*, 7890−7894.

(18) Seo, M.; Amendt, M. A.; Hillmyer, M. A. *Macromolecules* **2011**, *44*, 9310.